PERGAMON

Available online at www.sciencedirect.com

ScienceDirect

Acta Astronautica 63 (2008) 1169–1177

ACTA ASTRONAUTICA

www.elsevier.com/locate/actaastro

Dynamics and control of tethered satellite systems☆

A.K. Misra

McGill University, Montreal, QC, Canada H3A 2K6

Received 23 April 2007; accepted 25 June 2008
Available online 12 August 2008

Abstract

Dynamics and control of two-body and n-body tethered satellites are considered. At first, nonlinear roll and pitch motions of two-body systems are examined. Then the effects of aerodynamic and electrodynamic forces on the stability of a tethered satellite are discussed. Various control schemes to stabilize the dynamics during retrieval of the subsatellite are described. Finally, some dynamics and stability results for n-body tethered satellites are presented.

Keywords: Tethered satellites; Deployment/retrieval dynamics; Elastic oscillations

1. Introduction

There is a large body of literature dealing with the dynamics and control of tethered satellite systems. A survey of the early works in this area (until 1986) has been conducted by Misra and Modi [1]. A detailed analysis of various aspects of the dynamics of space tether systems can also be found in the excellent monograph by Beletsky and Levin [2], published in 1993. A lot of work has been done since then, in particular on nonlinear pitch and roll motion of tethered satellites, effect of aerodynamic and electrodynamic forces, dynamics of spinning tethered systems, control of tethered satellites, tether-assisted orbital transfer and dynamics of multi-tethered systems. The objective of this Breakwell Memorial Lecture is to discuss some of this recent work. This is not an exhaustive literature survey, but only an attempt to present some of the recent findings.

2. Nonlinear pitch and roll motions of tethered satellites

The equations governing the dynamics of tethered satellites are highly nonlinear. Hence the dynamical behavior is very rich and in some cases can be chaotic. The general dynamics of such systems involves pitch and roll motions of the tether, longitudinal and transverse elastic oscillations of the tether and three-dimensional attitude dynamics of the end-bodies. Pitch and roll motions of the tether are only marginally affected by the elastic oscillations of the tether and the rigid body dynamics of the end-bodies. Therefore, these two rotational motions can be investigated by modeling the system as one that consists of two point end-masses, m_1 and m_2, connected by a straight, rigid tether of length ℓ and mass m_t (Fig. 1). The equations governing the pitch angle α in the orbital plane (y-z plane) and roll angle γ

☆ The paper was presented as the Breakwell Memorial Lecture at the 54th International Astronautical Congress in Bremen, Germany in October 2003.

E-mail address: arun.misra@mcgill.ca.

0094-5765/$ - see front matter © 2008 Elsevier Ltd. All rights reserved.
doi:10.1016/j.actaastro.2008.06.020

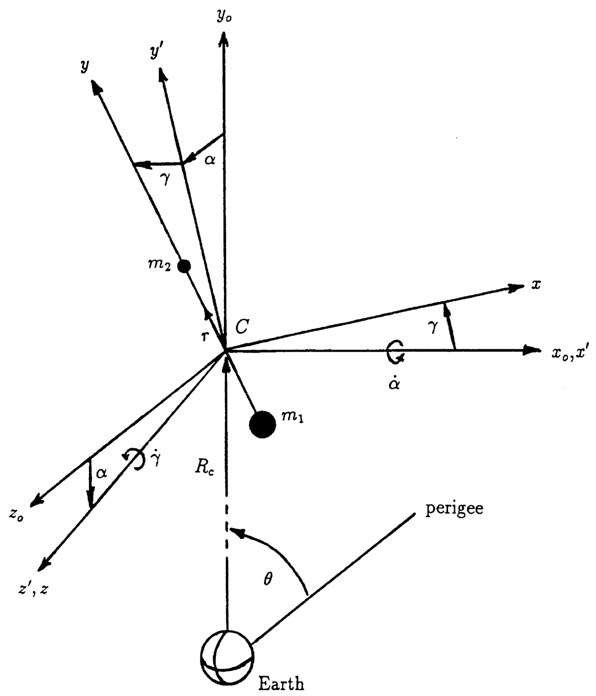

Fig. 1. Geometry of the system.

out-of-the orbital plane are then given by [3]

$$\cos^2\gamma[(\ddot{\alpha}+\ddot{\theta})+\{2r(\dot{\ell}/\ell)-2\dot{\gamma}\tan\gamma\}(\dot{\alpha}+\dot{\theta}) \\ +3(\mu/R_c^3)\sin\alpha\cos\alpha]=Q_\alpha/m_e\ell^2, \quad (1)$$

$$\ddot{\gamma}+2r(\dot{\ell}/\ell)\dot{\gamma}+[(\dot{\alpha}+\dot{\theta})^2+3(\mu/R_c^3)\cos^2\alpha]\sin\gamma\cos\gamma \\ =Q_\gamma/m_e\ell^2, \quad (2)$$

where Q_α and Q_γ are the generalized forces corresponding to α and γ, respectively, R_c and θ are radial distance of the centre of mass and true anomaly, respectively, while m_e and r are the equivalent mass of the system and a mass ratio, given by

$$m_e=[m_1m_2+(1/3)m_t(m_1+m_2) \\ +(1/12)m_t^2]/(m_1+m_2+m_t), \quad (3)$$

$$r=[m_1(m_2+(1/2)m_t)]/[m_1m_2+(1/3)m_t(m_1+m_2) \\ +(1/12)m_t^2]. \quad (4)$$

It is assumed here that the sequence of rotations is pitch angle α about the local vertical, followed by out-of-plane roll angle γ. It may be noted that, if the tether mass is small compared to the two end-masses, $m_e = m_1m_2/(m_1+m_2)$ and $r=1$.

For the convenience of analysis, the independent variable can be changed from time to true anomaly θ, in which case Eqs. (1) and (2) can be re-written as

$$\cos^2\gamma[\alpha''+\{2r(\ell'/\ell)-2\gamma'\tan\gamma-F\}(\alpha'+1) \\ +3G\sin\alpha\cos\alpha]=\bar{Q}_\alpha, \quad (5)$$

$$\gamma''+\{2r(\ell'/\ell)-F\}\gamma'+[(\alpha'+1)^2 \\ +3G\cos^2\alpha]\sin\gamma\cos\gamma=\overline{Q}_\gamma, \quad (6)$$

where prime denotes differentiation with respect to true anomaly θ, while F and G are functions of θ and eccentricity e as follows:

$$F=2e\sin\theta/(1+e\cos\theta), \quad G=1/(1+e\cos\theta). \quad (7)$$

Before studying the three-dimensional motions, the simpler planar case [3,4] is analyzed to form a comparison base. Assuming no external forces, Eq. (5) reduces to

$$\alpha''-F(\alpha'+1)+3G\sin\alpha\cos\alpha=0. \quad (8)$$

For the circular orbit case, Eq. (8) further reduces to

$$\alpha''+3\sin\alpha\cos\alpha=0. \quad (9)$$

The above equation is similar to that of a simple pendulum. The phase plane trajectories can be obtained by simple integration and are given by

$$\alpha'^2-3\cos^2\alpha=E, \quad (10)$$

where E is two times the Hamiltonian of the system. The separatrices ($E=0$) separate the libration ($E<0$) and tumbling ($E>0$) motions. The motion is always regular.

For the elliptic orbit case the equation of motion, Eq. (8), is non-autonomous and the phase space is spanned by the three dimensions α, α' and θ. The motion may be analyzed by taking a Poincaré section, i.e., sampling the states at the forcing frequency (orbital frequency) and plotting them in the α–α' plane. Such analysis shows that, when the eccentricity is increased, chaotic regions (represented by clouds of disorganized points) separating orderly librational and tumbling solutions appear (Fig. 2). The size of the chaotic region grows with eccentricity.

Coupled pitch–roll motion of tethered satellites show many interesting nonlinear features [3]. For the simpler case of circular orbits, the equations of motion for the unforced case are

$$\cos^2\gamma[\alpha''-2\gamma'\tan\gamma(\alpha'+1)+3\sin\alpha\cos\alpha]=0, \quad (11)$$

$$\gamma''+[(1+\alpha')^2+3\cos^2\alpha]\sin\gamma\cos\gamma=0. \quad (12)$$

The Hamiltonian of the system for the circular orbit case is constant and is given by

$$H=\tfrac{1}{2}n^2m_e\ell^2[\gamma'^2+\cos^2\gamma(\alpha'^2-1-3\cos^2\alpha)+1], \quad (13)$$

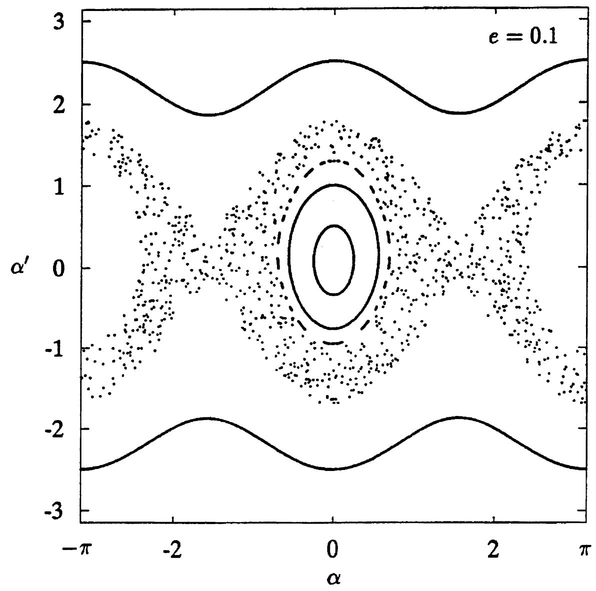

Fig. 2. Poincaré sections for planar motion for $e = 0.1$ (Ref. [3]).

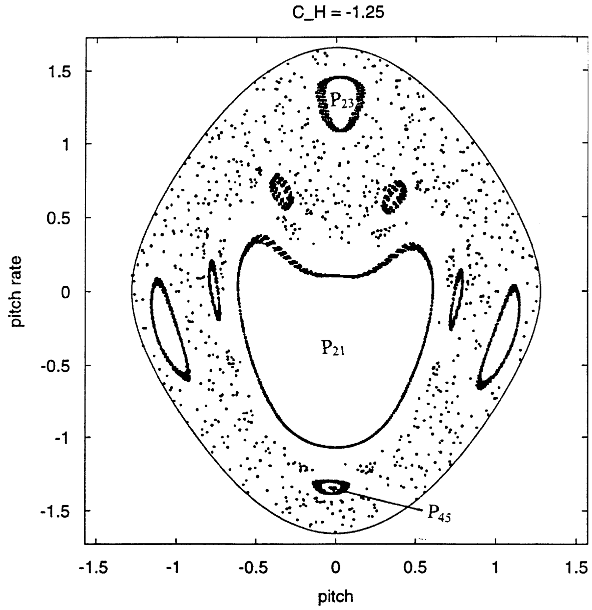

Fig. 3. Poincaré sections for coupled motion, circular orbit case for $C_H = -1.25$ (Ref. [3]).

where n is the orbital rate and m_e is as defined in Eq. (3). It is convenient to define a nondimensional Hamiltonian C_H as

$$C_H = (2H/n^2 m_e \ell^2) - 1 \\ = \gamma'^2 + \cos^2\gamma(\alpha'^2 - 1 - 3\cos^2\alpha). \tag{14}$$

For $C_H < -4$, no motion is possible; for $-4 \leqslant C_H \leqslant -1$, motion is bounded; for $-1 \leqslant C_H \leqslant 0$, motion is bounded in γ only; and for $0 < C_H$ unbounded motion (tumbling) can take place in both α and γ.

Fig. 3 presents Poincaré sections for $C_H = -1.25$, sampled for $\gamma = 0$. One can note islands of regular motion as well as chaotic motion depicted by a diffused set of points. The label P_{mn} signifies the existence of quasiperiodic solutions, m pitch oscillations in n roll oscillations. It has been observed that the region of chaotic motion increases with an increase in C_H. The nature of the motion can be examined further by applying the initial conditions $\alpha(0) = \gamma(0) = k$, $\alpha'(0) = \gamma'(0) = 0$ and gradually increasing k. For small values of k, say $10°$, the PSD is composed of combination tones of the two fundamental frequencies of the linearized system, $\sqrt{3}$ and 2 for pitch and roll, respectively. The PSD becomes broadband when k increases beyond $40°$ or so. Fig. 4 shows the behavior of the largest Lyapunov exponent λ when k is increased. λ tends to zero for $k \leqslant 42°$, but approaches a finite positive value when $k = 43°$, signifying the onset of chaos.

If the orbit is elliptic, both pitch and roll equations have time-varying coefficients. There are no equilibrium configurations and the Hamiltonian is not constant. Initial conditions can be applied similar to the circular case and Lyapunov exponents can be calculated. Fig. 5 shows the largest Lyapunov exponent for $k = 10°, 26°, 30°$ with $e = 0.1$. For $k \leqslant 26°$, the motion is found to be regular, λ approaching zero over time. However, for $k = 30°$, λ approaches a positive non-zero value implying chaotic motion. For the transition range, $k = 27°–28°$, weakly chaotic motion is observed.

3. Elastic oscillations of tethers

The tethers in tethered satellite systems are likely to undergo both longitudinal and transverse elastic oscillations. These oscillations are somewhat different from the standard string oscillations because the tether is subjected to a non-uniform axial tension generated due to the gravity–gradient and centrifugal force–gradient. In general, the longitudinal and transverse oscillations are coupled, but the coupling is weak in most cases.

The equation governing longitudinal oscillations of a tether, deployed from a large orbiter in a circular orbit, is given by [5]

$$EA\frac{\partial^2 u}{\partial s^2} - \rho\frac{\partial^2 u}{\partial t^2} + 3\rho\Omega^2(s + u) = 0, \tag{15}$$

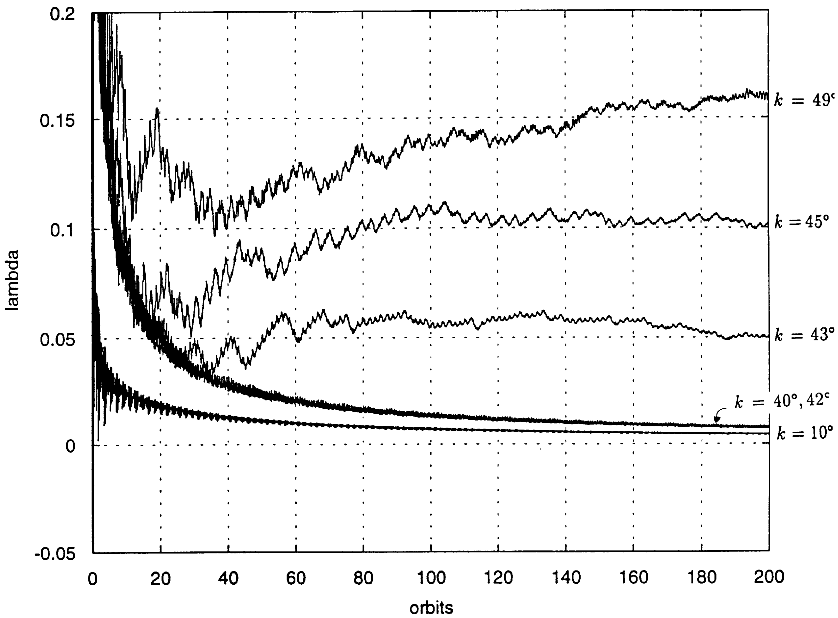

Fig. 4. Largest Lyapunov exponent for coupled motion, circular orbit case with $\alpha(0)=\gamma(0)=k$, $\alpha'(0)=\gamma'(0)=0$ (Ref. [3]).

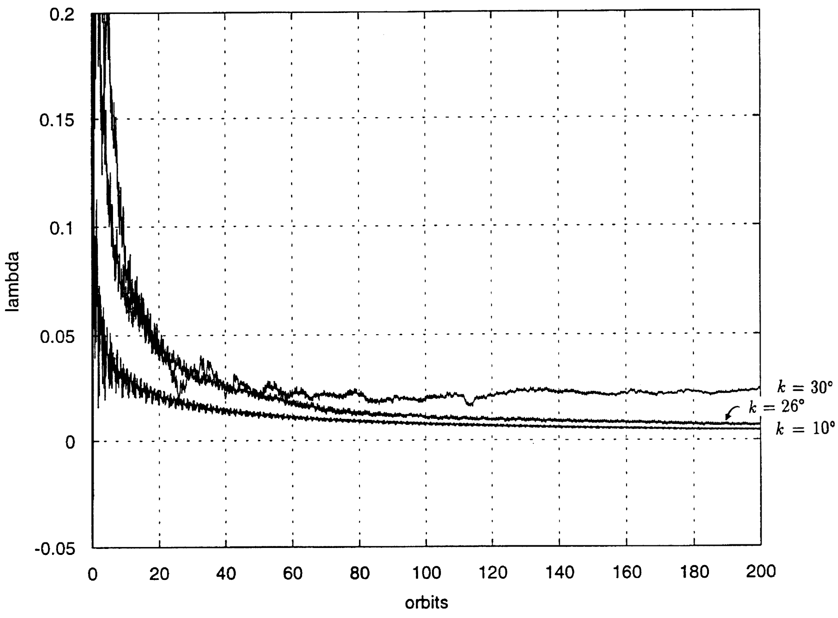

Fig. 5. Largest Lyapunov exponent for coupled motion, elliptic orbit case with $\alpha(0)=\gamma(0)=k$, $\alpha'(0)=\gamma'(0)=0$ and $e=0.1$ (Ref. [3]).

with the boundary conditions

$$u(o,t)=0,$$
$$-EA\frac{\partial u}{\partial s}(\ell_o,t)-m_2\frac{\partial^2 u}{\partial t^2}(\ell_o,t)+3m_2\Omega^2[\ell_o+u(\ell_o,t)]=0. \tag{16}$$

Here ℓ_o, A, E and ρ stand for the nominal length, area of cross-section, Young's modulus and mass per unit length of the tether, while $u(s,t)$ is the longitudinal displacement of an element of the tether located at a distance s from the orbiter. Ω is the angular velocity of the orbiter in the circular orbit. Eq. (15), with boundary conditions (16), can be solved analytically [5]. The solution contains a static extension and an oscillatory component. The steady state tension can be written approximately as

$$T_o = 3m_2\Omega^2\ell_o[1 + (1/2)(m_t/m_2)(1 - s^2/\ell_o^2)], \quad (17)$$

i.e., it varies quadratically along the length. The frequency equation can be written as

$$\beta \tan\beta = (m_t/m_2), \quad (18)$$

where

$$\beta = (3 + \lambda^2)^{1/2}(\rho\ell_o^2/EA)^{1/2}\Omega, \quad (19)$$

λ being the longitudinal frequency nondimensionalized with respect to Ω. It has been observed that the lowest root λ_1 obtained from the solution of Eqs. (18) and (19) varies as ${\ell_o}^{-1/2}$, while the rest of the roots vary as ℓ_o^{-1}. Furthermore, only the lowest longitudinal frequency is affected by the mass of the subsatellite; the others are not affected very much.

The equations governing the transverse vibrations are

$$\rho\frac{\partial^2 v}{\partial t^2} - \frac{\partial}{\partial s}\left(T_o\frac{\partial v}{\partial s}\right) = 0, \quad (20)$$

$$\rho\frac{\partial^2 w}{\partial t^2} - \frac{\partial}{\partial s}\left(T_o\frac{\partial w}{\partial s}\right) - \Omega^2 w = 0, \quad (21)$$

with boundary conditions $v(o,t) = v(\ell_o,t) = w(o,t) = w(\ell_o,t) = 0$. Here $v(s,t)$ and $w(s,t)$ are the transverse displacements in the orbital plane and perpendicular to the orbital plane, respectively. T_o is the steady state tension given by Eq. (17).

Frequencies of in-plane and out-of-plane transverse oscillations can be determined by solving Eqs. (20) and (21), respectively. The in-plane frequencies can be shown to be given by

$$\omega_{n_I} = \beta_n(3m_2/m_t)^{1/2}\Omega, \quad (22)$$

where

$$\beta_n^2 = n^2\pi^2[1 + (m_t/3m_2)] - (m_t/4m_2). \quad (23)$$

The out-of-plane frequencies are related to the in-plane frequencies by

$$\omega_{n_o}^2 = \omega_{n_I}^2 + \Omega^2. \quad (24)$$

4. Effect of aerodynamic and electrodynamic forces

The most important external forces on a tethered satellite system are the gravitational forces, solar radiation pressure, aerodynamic forces and electrodynamic forces. The gravitational perturbations due to the oblateness of the earth are of relatively minor importance for tethered satellites. Similarly for low altitude orbits, the effects of solar radiation pressure on the dynamics are not very significant except that temperature variation can cause longitudinal oscillations. On the other hand, aerodynamic and electrodynamic forces can affect the stability of the system significantly under certain circumstances.

Aerodynamic forces can drastically modify the trajectory of satellites in LEO. The most important consideration for tethered satellites in this regard is the orbital decay and the estimate of the lifetime of tethered systems. As one will expect, the lifetime depends on whether the system is a free tether, a single satellite trailing a tether or a tethered two-body system. It is important to consider the oblateness of the earth, rotation of the atmosphere as well as temporal and spatial variation of the atmospheric density to obtain an accurate estimate of the lifetime. An excellent treatment of this topic can be found in the paper by Warnock and Cochran [6]. The lifetime is strongly dependent on the length of the tether and the perigee height; a sample result from Ref. [6] for a free tether is given in Fig. 6.

Aerodynamic forces can affect the librational motion of a tethered satellite system significantly. Onada and Watanabe [7] showed that uncontrolled motion of a spherical sub-satellite deployed into a region where the atmospheric density is significant can be unstable due to the combined effects of atmospheric density gradient and extensional oscillation of the tether. Keshmiri et al. [8] showed that aerodynamic lift can have a significant effect as well; in fact, librations of an unstable system with a spherical subsatellite can be stabilized if an appropriate lifting surface is added. A lifting surface can also be used for active altitude control of an atmospheric probe, as shown by Biswell and Puig-Suari [9].

Tethers can also be used for aerobraking in planetary missions. Detailed studies of various issues associated with tether-assisted aerobraking have been conducted by Longuski et al. (see for example, Ref. [10]).

The motion of a conductive wire across the magnetic field of the earth induces an emf and a Lorentz force across the system. The resulting voltage and force can provide electrical power and control the motion of a spacecraft. This "electrodynamic propulsion" can be used to raise or change the orbit of a spacecraft, or for removal of orbital debris. In the former case the tether acts as a thruster that converts electrical energy into orbital energy, while in the latter case the tether

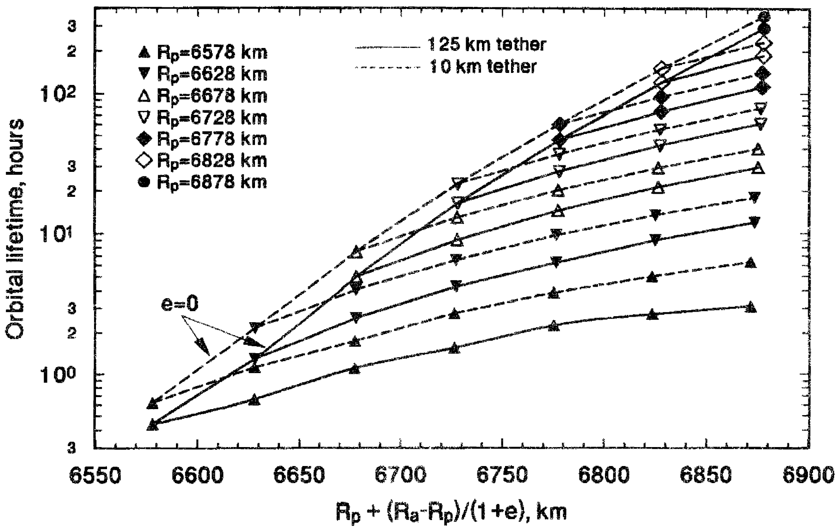

Fig. 6. Free tether orbital lifetime prediction curves (Ref. [5]).

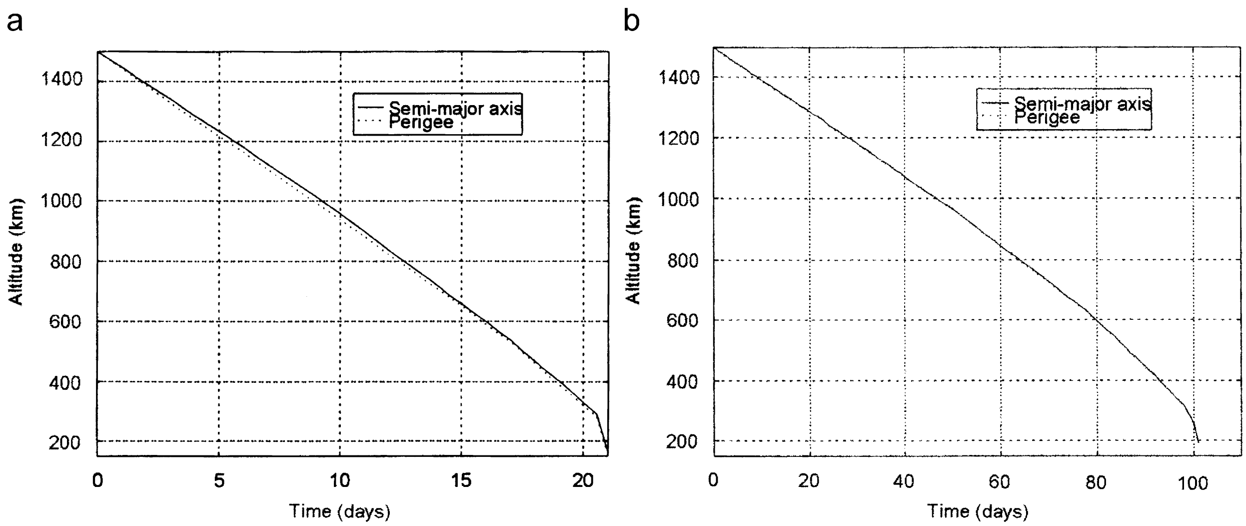

Fig. 7. Orbital decay for circular orbit at 1500 km; (a) $i = 0°$ and (b) $i = 85°$ (Ref. [13]).

converts orbital energy into electrical energy. Excellent treatment of this topic can be found in Martínez-Sánchez and Hastings [11], Estes et al. [12] and Lanoix et al. [13]. Use of an electrodynamic tether for orbital decay is much more efficient for an equatorial orbit than for nearly polar orbits (Fig. 7).

Pitch and roll motions of the tether are significantly affected by electrodynamic forces. Peláez et al. [14,15] have shown that pitch and roll instability arises for inclined orbits, both in the circular and in the elliptic cases, since the electrodynamic forces pump energy continuously into the system.

5. Deployment and retrieval

During deployment or retrieval of a tethered subsatellite, the length of the tether varies with time and the equations of motion are much more complex. The coupled pitch and roll motions are governed by Eqs. (5) and (6). To understand the basic behavior, let us consider small motion, small tether mass and a circular orbit. The equations of motion in the absence of external forces then reduce to

$$\alpha'' + 2(\ell'/\ell)\alpha' + 3\alpha = -2(\ell'/\ell), \tag{25}$$

$$\gamma'' + 2(\ell'/\ell)\gamma' + 4\gamma = 0. \tag{26}$$

It may be noted that both pitch and roll angles have damping terms proportional to ℓ'/ℓ. During deployment, ℓ'/ℓ is positive and the motion tends to be stable. During retrieval, on the other hand, ℓ'/ℓ is negative and the motion is unstable.

Since uncontrolled dynamics during retrieval is unstable, a lot of effort has gone into developing control schemes to stabilize the dynamics. The control can be implemented by modulating the tension [16–18] or reel rate [18,19], by applying thrusters [20,21], or by moving the point of attachment of the tether [22]. The first attempt to control the system dynamics during deployment or retrieval was made by Rupp who proposed the tension in the tether to be modulated in the form

$$T = K_1\ell + C_1\dot{\ell} + K_2\ell_c, \tag{27}$$

where ℓ and $\dot{\ell}$ are instantaneous length and length rate, respectively, ℓ_c is a commanded length, while K_1, K_2 and C_1 are a set of constants. The gains were modified later [16] to improve the control performance, i.e., the tension was applied in the form

$$T = [m_2 + (1/2)m_t][(R^2+3)\Omega^2\ell + 2\zeta_c R\Omega\dot{\ell} - R^2\Omega^2\ell_c], \tag{28}$$

where R is an imposed ratio (around 2) between the control law stretch frequency and orbital frequency, while ζ_c is the control damping.

Bainum and Kumar [17] have proposed an optimal control law of the form

$$T = T_o + K_\ell\hat{\ell} + K_{\ell'}\hat{\ell}' + K_\alpha\alpha + K_{\alpha'}\alpha', \tag{29}$$

where $\hat{\ell}$ is the nondimensional difference between the actual and the commanded tether length ($\hat{\ell} = \ell/\ell_c - 1$).

The control laws (28) and (29) work well for the in-plane motion, but not so well for the out-of-plane motion. Nonlinear control strategies must be used for keeping the three-dimensional motion bounded. Modi et al. [18] have proposed tension modulation of the form

$$T = T_o + K_\ell\ell + K_{\ell'}\ell' + K_\gamma\gamma'^2, \tag{30}$$

and tether reel control laws

$$\ell'/\ell = K_\theta(1 - K_\alpha\alpha' - K_\gamma\gamma'^2), \tag{31}$$

which seem to work quite well. Optimal feedback tether reel control laws to control deployment/retrieval have also been developed by Williams et al. [23].

Electrodynamic forces can also be used to control the tether pitch and roll; Williams [24] has done this for the deployment case, but the approach can be adapted to retrieval as well. Hybrid schemes involving two or more of the above-mentioned approaches have also been used [25]. Fig. 8 shows the response for one such scheme that combines offset and thruster control.

The control laws can be obtained using a pole-placement technique or the LQR method. Several laws based on Lyapunov method (or a variant) have also been devised [26,27].

6. Multi-tethered systems

Interest in multi-tethered systems was initially related to the deployment of multiple probes from a spacecraft to the upper atmosphere and for microgravity applications. These systems were modeled as an open chain of tether-connected bodies. Lorenzini [19] studied the in-plane dynamics of a three-body tethered system and proposed schemes to control its motion. Misra et al. [28–30] considered n-body systems in detail numerically and three-body systems analytically. It was shown [28] that the in-plane librational frequencies of an open-chain n-body system in a circular orbit can be obtained by solving the eigenvalue problem $[K]\{x\} = \omega^2[M]\{x\}$, where the elements of $[M]$ are given by

$$M_{jk} = G_{jk}\ell_j\ell_k, \tag{32}$$

and those of $[K]$ are given by

$$K_{jj} = 3\Omega^2\sum_{p=1}^{N-1} M_{jp}, \quad K_{jk} = 0 \text{ for } j \neq k. \tag{33}$$

In Eq. (32), ℓ_j and ℓ_k are lengths of the jth and kth tether, respectively, while G_{jk} is a function of mass ratios given in Ref. [28]. In Eq. (33), Ω is the orbital angular velocity. It was noted that the in-plane and out-of-plane librational frequencies are related by (for the circular orbit case)

$$\omega_{oj}^2 = \omega_{Ij}^2 + \Omega^2, \tag{34}$$

where Ω is the orbital frequency. Control laws were also proposed and elastic frequencies were calculated.

Analysis of the motion of a three-body system showed that there are many equilibrium configurations, some triangular and some collinear [30]. All triangular configurations are unstable and only one collinear configuration is stable.

There is currently a lot of interest in tethered satellite formations because of their possible application in remote sensing and space interferometry. These may have some advantages over free satellite formations as far as relative station-keeping is concerned. Tragesser

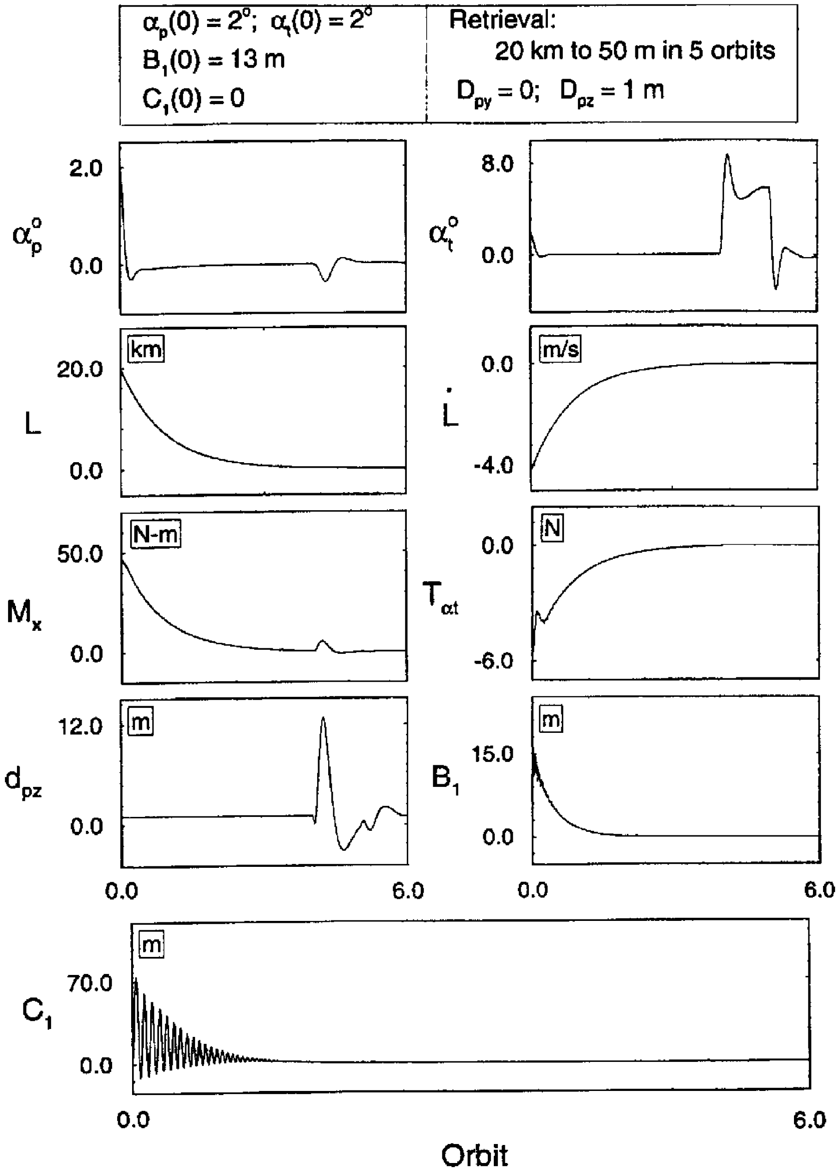

Fig. 8. Retrieval dynamics during a hybrid control strategy (Ref. [25]).

and Tuncay [31] and Williams and Moore [32] have considered the feasibility and stability of various configurations such as ring, hub-spoke and gravity–gradient anchored configurations. They have also determined the tension requirements in various configurations. However, these studies have not considered many issues dealing with the dynamics of the tethers.

Bombardelli et al. [33,34] have investigated the pointing dynamics and retargeting dynamics of tethered formations for space interferometry. Another interesting study is that of the dynamics of a tethered satellite formation located at a libration point of the Sun–Earth system [35]; pointing control of such systems have been attempted with some success.

Control of tethered satellite formations is a challenging problem and is an active area of research at present.

7. Conclusion

There is considerable wealth of literature dealing with the dynamics and control of tethered satellite systems. The state of art is reviewed briefly in this paper. It is not an exhaustive review and to some extent has a disproportionate focus on the work done by this author.

The area in which a lot of additional effort is needed is the one dealing with the dynamics and control of tethered satellite formations, taking into account the librations and elastic oscillations of the tethers.

References

[1] A.K. Misra, V.J. Modi, A survey on the dynamics and control of tethered satellite systems, Advances in Astronautical Sciences 62 (1987) 667–719.

[2] V.V. Beletsky, E.M. Levin, Dynamics of space tether systems, Advances in Astronautical Sciences 83 (1993).

[3] A.K. Misra, M.S. Nixon, V.J. Modi, Nonlinear dynamics of two-body tethered satellite systems: constant length case, Journal of Astronautical Sciences 49 (2001) 219–236.

[4] H.A. Fujii, W. Ichiki, Nonlinear dynamics of the tethered subsatellite system in the stationkeeping phase, Journal of Guidance Control and Dynamics 20 (1997) 403–406.

[5] A.K. Misra, V.J. Modi, Extensional oscillations of tethered satellite systems, Journal of Guidance Control and Dynamics 11 (1988) 594–596.

[6] T.W. Warnock, J.E. Cochran Jr., Orbital life time of tethered satellites, Journal of Astronautical Sciences 41 (1993) 165–188.

[7] J. Onada, N. Watanabe, Tethered subsatellite swinging from atmospheric gradient, Journal of Guidance Control and Dynamics 11 (1988) 477–479.

[8] M. Keshmiri, A.K. Misra, V.J. Modi, Effects of aerodynamic lift on the stability of tethered satellite systems, Journal of Astronautical Sciences 42 (1994) 301–318.

[9] B.L. Biswell, J. Puig-Suari, Altitude control of a tethered lifting probe for atmospheric research, Journal of Astronautical Sciences 49 (2001) 283–307.

[10] J.M. Longuski, J. Puig-Suari, J. Mechalas, Aerobraking tethers for the exploration of the solar system, Acta Astronautical 35 (1995) 205–214.

[11] M. Martínez-Sánchez, D.E. Hastings, A systems study of a 100 kW electrodynamic tether, Journal of Astronautical Sciences 35 (1987) 75–96.

[12] R.D. Estes, E.C. Lorenzini, J.R. Sanmartín, J. Peláez, M. Martínez-Sánchez, L. Johnson, I. Vas, Bare tethers for electrodynamic spacecraft propulsion, Journal of Spacecraft and Rockets 37 (2000) 205–211.

[13] E.L.M. Lanoix, A.K. Misra, V.J. Modi, G. Tyc, Effect of electromagnetic forces on orbital dynamics of tethered satellites, in: AAS/AIAA Spaceflight Mechanics Meeting, Clearwater, Florida, Paper No. AAS-00-189, 2000.

[14] J. Peláez, E.C. Lorenzini, O. López-Rebollal, M. Ruiz, A new kind of dynamic instability in electrodynamic tethers, Journal of Astronautical Sciences 48 (2000) 449–476.

[15] J. Peláez, Y.N. Andrés, Dynamic stability of electrodynamic tethers in inclined elliptical orbits, in: AAS/AIAA Astrodynamic Specialists Conference, Big Sky, Montana, Paper No. AAS-03-538, 2003.

[16] W.P. Baker, et al., Tethered subsatellite study, Technical Report NASA TMX-73314, Marshal Space Flight Center, Alabama, AL, USA, 1976.

[17] P.M. Bainum, V.K. Kumar, Optimal control of the shuttle-tethered system, Acta Astronautica 7 (1980) 1333–1348.

[18] V.J. Modi, G. Chang-fu, A.K. Misra, D.M. Xu, On the control of the space shuttle based tethered system, Acta Astronautica 9 (1982) 437–443.

[19] E.C. Lorenzini, A three-mass tethered system for micro-*g*/variable-*g* applications, Journal of Guidance Control and Dynamics 10 (1987) 242–249.

[20] A.K. Banerjee, T.R. Kane, Tethered satellite retrieval with thruster augmented control, Journal of Guidance Control and Dynamics 9 (1984) 663–672.

[21] D.M. Xu, A.K. Misra, V.J. Modi, Thruster-augmented active control of a tethered subsatellite system during its retrieval, Journal of Guidance Control and Dynamics 9 (1986) 663–672.

[22] V.J. Modi, P.K. Lakshmanan, A.K. Misra, Offset control of tethered satellite systems: analysis and experimental verification, Acta Astronautica 21 (1990) 283–294.

[23] P. Williams, C. Blanksby, P. Trivailo, H.A. Fujii, In-plane payload capture using tethered, Acta Astronautica 57 (2005) 772–787.

[24] P. Williams, C. Blanksby, P. Trivailo, The use of electromagnetic Lorentz forces as a tether control actuator, in: 53rd International Astronautical Congress, Houston, Texas, Paper No. IAC-02-A.5.04, 2002.

[25] V.J. Modi, S. Pradhan, A.K. Misra, Controlled dynamics of flexible orbiting tethered systems, Journal of Vibration and Control 3 (1997) 459–497.

[26] S.R. Vadali, E.S. Kim, Feedback control of tethered satellites using Lyapunov stability theory, Journal of Guidance Control and Dynamics 14 (1991) 729–735.

[27] H.A. Fujii, K. Uchiyama, K. Kokubun, Mission function control of tethered subsatellite deployment/retrieval: in-plane and out-of-plane motion, Journal of Guidance Control and Dynamics 14 (1991) 471–473.

[28] A.K. Misra, V.J. Modi, Three-dimensional dynamics and control of tether-connected N-body systems, Acta Astronautica 26 (1992) 77–84.

[29] M. Keshmiri, A.K. Misra, V.J. Modi, General formulation for N-body tethered satellite system dynamics, Journal of Guidance Control and Dynamics 19 (1996) 75–83.

[30] A.K. Misra, Equilibrium configurations of tethered three-body systems and their stability, Journal of Astronautical Sciences 50 (2002) 241–253.

[31] S.G. Tragesser, A. Tuncay, Orbital design of Earth—oriented tethered satellite formations, Journal of Astronautical Sciences 53 (2005).

[32] T. Williams, K. Moore, Dynamics of tethered satellite formations, in: AAS/AIAA Space Flight Mechanics Meeting, San Antonio, Texas, Paper No. AAS-02-198, 2002.

[33] C. Bombardelli, E.C. Lorenzini, M.B. Quadrelli, Formation pointing dynamics of tether-connected architecture for space interferometry, Journal of Astronautical Sciences 52 (2004) 475–493.

[34] C. Bombardelli, E.C. Lorenzini, M.B. Quadrelli, Retargeting dynamics of a linear tethered interferometer, Journal of Guidance Control and Dynamics 27 (2004) 1061–1067.

[35] B. Wong, A.K. Misra, Dynamics of Lagrangian point multi-tethered satellite systems, Journal of Astronautical Sciences 53 (2005) 221–250.